ELECTRONIC PROPERTIES OF PSEUDOMORPHIC InGaAs/AlGaAs (ON GaAs) AND InGaAs/InAlAs (ON InP) MODFET STRUCTURES.

Mark Jaffe, Yoshihiko Sekiguchi, Jack East and Jasprit Singh
Center for High Frequency Microelectronics
Department of Electrical Engineering and Computer Science
The University of Michigan
Ann Arbor, Michigan 48109

(Received 17 August 1987)

Pseudomorphic (strained channel) modulation doped field effect transistors (MODFETs) have recently received a considerable amount of attention. These devices provide potential for both improved device performance and new physics studies. In this paper we present theoretical studies of n-type and p-type strained channel MODFETs. Information on carrier masses, subband occupation, and the charge control picture as a function of strain in the channel is presented. The n-MODFET studies are based on using the results of tight binding calculations for bandstructure in the strained channel. The p-MODFET problem involves the use of the Kohn Luttinger hamiltonian. Self consistent solution of the Schrödinger equation and the Poisson equation then allows us to study the MODFET properties. In p-type MODFETs, the control of heavy hole - light hole coupling via strain allows the possibility of tailoring hole masses. Comparisons with some of the experimental works previously published are also presented.

I. INTRODUCTION

In a few short years, advances in epitaxial growth techniques such as molecular beam epitaxy (MBE) and metal-organic chemical vapor deposition (MOCVD) have moved the MODFET from a research curiosity to a commercially viable device. Much of the MODFET work has focused on material systems composed of GaAs/AlGaAs (on GaAs substrates), and more recently, $In_{0.53}Ga_{0.47}As$/-$In_{0.52}Al_{0.48}As$ (on InP substrates). These are lattice matched systems with relatively well developed growth and processing technologies.

In general, the device performance of a MODFET can be improved by controlling the following material related issues: i) higher sheet charge density (controlled by increasing the band discontinuity), ii) lower carrier effective mass (by altering the channel bandstructure), iii) increasing peak and saturation velocities (by increasing band discontinuity and intervalley separation), iv) increasing low field mobility (by lighter carrier effective masses and better carrier confinement). It is possible to achieve the above goals by introducing excess In in the channels of the two lattice matched systems mentioned above. For the GaAs/AlGaAs system, addition of In could also avoid the light sensitivity problem that the n-type lattice matched system suffers from[1]. The use of strain in p-MODFETs can have additional advantages due to the ability of strain to decrease the hole masses. Indeed, recently, p-MODFETs have received considerable attention due to this potential. The need for superior hole transport properties exists for both p-MODFETs (for complimentary logic) and for npn heterojunction bipolar transistors (HBTs). Work by Jones et al[2] on the InGaAs/GaAs structure has shown that hole masses can indeed be decreased by biaxial compressive strain. Strained p-MODFETs have been studied by Drummond et al[3] and Lee et al[4] with both groups finding enhanced device performance due to strain.

To fully exploit the potential of strained channel MODFETs, it is important to develop a formalism to study the channel material properties and charge control properties of both n-type and p-type devices. An accurate formalism tested against relevant experiments can then allow an optimization of such devices. In this paper, we provide a formalism based upon accurate numerical techniques to study the full quantum mechanical problem of the n- and the p-MODFET. The p-MODFET requires a formalism which is capable of treat-

0749–6036/88/040395 + 10 $02.00/0

© 1988 Academic Press Limited

ing the heavy hole (HH) - light hole (LH) problem self consistently with the Poisson equation. Such a formalism along with the techniques necessary to solve it are presented as well.

In the next section, we present the theoretical formalism necessary to understand the charge control picture in n- and p-type MODFETs. The results of the modeling are presented in section III, after which we conclude in section IV.

II. THEORETICAL CONSIDERATIONS

The general strained channel MODFET is shown in figure 1 where excess In is added in the channel where the two dimensional electron (hole) gas is formed. Before the MODFET properties are understood, it is important to study the bandstructure of the strained region. Once the bandstructure in known, one must solve the relevant Schrödinger equation self consistently with the Poisson equation. The formalism must be capable of dealing with arbitrary layer properties and shapes of the potential profile in the well region and, therefore, we do not employ the variational technique for solution of the Schrödinger equation which has been employed commonly in modeling the lattice matched MODFET.

In figure 2, we depict the general flowchart of our approach to n- and p-type MODFET simulation. We now describe the components of our formalism.

II.a Bandstructure of the Strained Channel Region

Formalism for n-MODFET:

We have used the tight binding method (TBM), in order to model the carrier masses in the strained channel. The bandstructure is developed first for the unstrained channel material by carefully fitting the bandgap, effective masses, and intervalley separations. THe effects of spin-orbit interaction are included in the tight binding formalism[5]. The virtual crystal approximation is employed to model alloys by averaging the tight binding matrix elements. This yields a set of tight binding matrix elements (and spin-orbit coupling parameters) which accurately describe the bandstructure to about 1 eV away from the bandgap for both the electron and the hole states.

After the tight binding parameter set for the channel material is developed, the effects of strain on the tight binding bandstructure are considered. Known deformation potentials of the material are fit by developing a scaling model for the tight binding matrix elements with strain-altered interatomic distances. A scaled square law

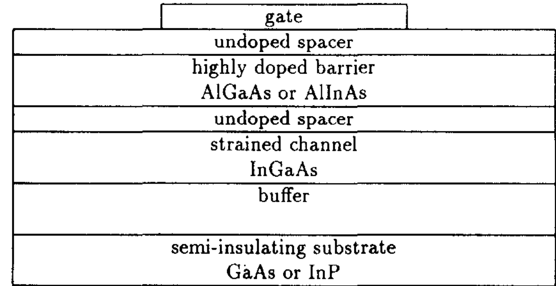

Figure 1: General structure of the pseudomorphic MODFET.

rule is used alter the tight binding matrix elements with the change in atomic separation[6]. Our formalism used the following relation

$$E_{\mu,\mu'}(r_o+\delta r) = \frac{E_{\mu,\mu'}(r_o)}{1 + \alpha\left(\frac{2\delta r}{r_o} + \frac{\delta r^2}{r_o^2}\right)} \quad (1)$$

Here μ and μ' stand for atomic orbitals (s, p_x, p_y, p_z) at sites which in the absence of strain are separated by a distance r_o. δr is the change in the atomic spacing and α is a fitting factor used to match the calculated deformation potentials for hydrostatic and biaxial deformation to measured values. Different values for alpha were used for first and second nearest neighbor interactions[**]. This expression, when incorporated into the tight binding formalism, allows one to describe the energy bandstructure under arbitrary strain conditions.

Using this formalism, we can determine the bandstructure of the strained channel for a given model for the absorption of the strain by the system. We employ the pseudomorphic approximation for strain incorporation in the channel material. According to this approximation, the lattice constant of the regions matched to the substrate is unaffected. In the non-matched region, the parallel lattice constant is forced to take on the value of the lattice constant of the substrate, while the perpendicular lattice constant of the non-matched material is then altered according to the Poisson effect. Thus, the parallel and perpendicular lattice constants of the strained channel become

$$\begin{aligned} a_{\parallel}^c &= a_o^s \quad (2)\\ &= (1+\varepsilon)a_o^c \\ a_{\perp}^c &= (1-\sigma\varepsilon)a_o^c \quad (3)\end{aligned}$$

where a_o represents an unstrained material lattice constant, the superscript 'c' denotes the channel material, the superscript 's' denotes the substrate material, and σ is Poisson's ratio for the channel material.

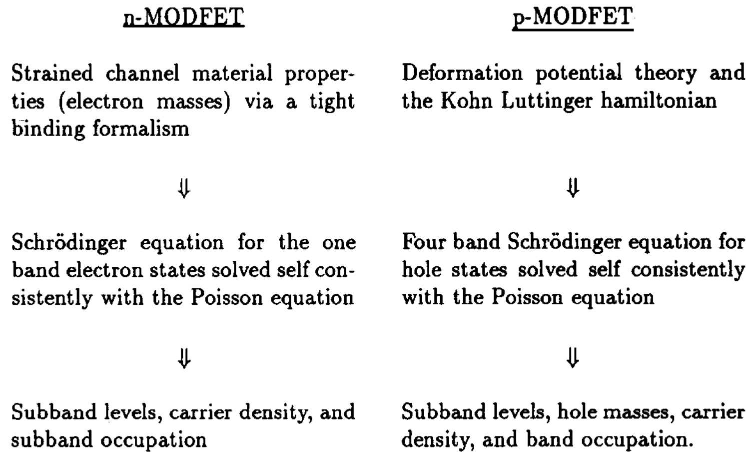

Figure 2: Flow chart modeling the procedure for n- and p-type pseudomorphic MODFETs.

Table 1: Band gaps of pseudomorphically strained channel materials on GaAs and InP substrates.

x	$In_xGa_{1-x}As$		$In_{0.53+x}Ga_{0.47-x}As$	
	$E_{gap-unstrained}$	$E_{gap-strained}$	$E_{gap-unstrained}$	$E_{gap-strained}$
0.00	1.4540	1.4540	0.8759	0.8759
0.03	1.4211	1.4337	0.8435	0.8527
0.06	1.3881	1.4132	0.8111	0.8287
0.09	1.3552	1.3924	0.7787	0.8039
0.12	1.3223	1.3714	0.7463	0.7785

Table 2: Effective masses in the perpendicular and parallel direction for pseudomorphically strained channel materials on GaAs and InP substrates.

x	$In_xGa_{1-x}As$			$In_{0.53+x}Ga_{0.47-x}As$		
	$m^*_{unstrained}$	$m^*_{\parallel strained}$	$m^*_{\perp strained}$	$m^*_{unstrained}$	$m^*_{\parallel strained}$	$m^*_{\perp strained}$
0.00	0.0660	0.0660	0.0660	0.0457	0.0457	0.0457
0.03	0.0648	0.0656	0.0652	0.0446	0.0451	0.0455
0.06	0.0636	0.0651	0.0646	0.0434	0.0444	0.0453
0.09	0.0624	0.0647	0.0639	0.0423	0.0437	0.0451
0.12	0.0612	0.0642	0.0634	0.0411	0.0429	0.0449

In tables 1 and 2, we show some calculated values of the electron properties in channel materials lattice matched to GaAs and InP substrates. Note that table 2 gives values of the effective mass in the parallel and the perpendicular directions for the strained channel materials. For unstrained materials, the equi-energy surfaces for the gamma valley are spherical in the materials which we are considering. Strain, however, lowers the symmetry of the crystal and changes the shape of the equi-energy surfaces to elipsoidal. That is, the biaxially strained gamma valley must be characterized by a parallel and a perpendicular effective mass which will, in general, be different.

Formalism for p-MODFET:

The plan of attack for modeling p-type MODFETs must be different then for the n-type devices. This is because the hole bands couple to each other, and this coupling is effected by the shape of the confining po-

tential. The inter-band coupling strongly controls the k-space dispersion of the bands, and thus alters the effective mass in the parallel directions. This is different from the n-type case where we assumed that the parallel effective mass was a material property which was uneffected be the confining potential in the 'z' direction. To model the subband dispersion in a p-type strained MODFET, we use the Kohn Luttinger hamiltonian. This method is useful since it can be directly used to set up the Schrödinger equation for the hole envelope function in the MODFET geometry.

Before examining confined hole bandstructures, one first must understand the Kohn Luttinger model for the valence bandstructure in bulk materials. The four band hamiltonian describes the bulk hole states quite accurately up to several hundred meV below the top of the valence band. For bulk material, the Kohn Luttinger Hamiltonian can be written as[7]

$$\begin{bmatrix} H_{hh} & c & b & 0 \\ c^* & H_{lh} & 0 & -b \\ b^* & 0 & H_{lh} & c \\ 0 & -b^* & c^* & H_{hh} \end{bmatrix} \begin{bmatrix} \Phi_{\frac{3}{2}\frac{3}{2}} \\ \Phi_{\frac{3}{2}\frac{1}{2}} \\ \Phi_{\frac{3}{2}\frac{-1}{2}} \\ \Phi_{\frac{3}{2}\frac{-3}{2}} \end{bmatrix} = E \begin{bmatrix} \Phi_{\frac{3}{2}\frac{3}{2}} \\ \Phi_{\frac{3}{2}\frac{1}{2}} \\ \Phi_{\frac{3}{2}\frac{-1}{2}} \\ \Phi_{\frac{3}{2}\frac{-3}{2}} \end{bmatrix} \quad (4)$$

where

$$\begin{aligned} H_{hh} &= -\frac{\hbar^2}{2m_o}\left[(k_x^2+k_y^2)(\gamma_1+\gamma_2) + k_z^2(\gamma_1-2\gamma_2)\right] \\ H_{lh} &= -\frac{\hbar^2}{2m_o}\left[(k_x^2+k_y^2)(\gamma_1-\gamma_2) + k_z^2(\gamma_1+2\gamma_2)\right] \\ c &= \frac{\sqrt{3}\hbar^2}{2m_o}\left[\gamma_2(k_x^2-k_y^2) - 2i\gamma_3 k_x k_y\right] \\ b &= \frac{\sqrt{3}\hbar^2}{m_o}(k_x - ik_y)\gamma_3 k_z \end{aligned} \quad (5)$$

Here, γ_1, γ_2 and γ_3 are the Luttinger parameters. These parameters determine the band interaction, and are generally considered to be a material characteristic. Parameters for many different III-V semiconductors are given by Lawaetz[8]. In the case of alloys, we used an average of the parameters which Lawaetz listed for the pure compounds.

The effect of biaxial strain on the hole bandstructure is to cause a splitting between the heavy and the light hole states. This splitting is given by

$$\begin{aligned} HeavyHole: \ E_{HH} &= E_o + \frac{1}{2}\delta_{sh} - \delta_{hy} \\ LightHole: \ E_{LH} &= E_o - \frac{1}{2}\delta_{sh} - \delta_{hy} \end{aligned} \quad (6)$$

Here δ_{sh} and δ_{hy} are the shear and the hydrostatic contributions to the change in the band energies from the unstrained energy, E_o, and are given by:

$$\begin{aligned} \delta_{sh} &= -2b\left[(c_{11}+2c_{12})/c_{11}\right]\varepsilon \\ \delta_{hy} &= -2a\left[(c_{11}-c_{12})/c_{11}\right]\varepsilon. \end{aligned} \quad (7)$$

c_{11} and c_{12} are the elastic parameters of the channel material, ε is the strain in the parallel direction, and a and b are the material deformation potentials. For $In_xGa_{1-x}As$ the experimentally measured material properties yield a shift of -5.96·ε for the heavy hole band and -12.4·ε for the light hole band[9].

To describe the hole states in a biaxially strained region, one can simply include the splitting between the HH and LH states in the diagonal terms of the Hamiltonian. The inclusion of this splitting alters the extent of the coupling between the HH and the LH states, and therefore changes the hole masses in the perpendicular and the parallel (or the transport) directions.

II.b Subband dispersion relations in a MODFET

The next step in the calculation is to obtain the band dispersion relations in the quantum well which confines the carriers in the MODFET. This requires a self consistent solution of the Poisson equation which establishes the potential profile in the MODFET, and the Schrödinger equation.

A technique commonly used to solve the Schrödinger equation is the variational approach. While this is a useful technique and can involve considerable savings in computer time, it is not possible to apply it to arbitrary shaped potentials with material parameters which change considerably across interfaces. We solve the problem numerically by casting the Schrödinger equation as a finite difference equation which is solved by using standard eigen system solution routines commonly available in computer mathematics libraries. This is possible since we are only interested in bound or quasi bound states. Therefore, without loss of generality, we can apply the boundary condition $\Psi(-L) = \Psi(L) = 0$. Here, $\pm L$ is the region surrounding the well in which the two dimensional electron gas is formed.

The Schrödinger equation for the one band electron problem is written as:

$$-\frac{\hbar^2}{2\overline{\overline{m}}^*}\nabla^2\Psi_n(\mathbf{k}_{\|}, z) + V(z)\Psi_n(\mathbf{k}_{\|}, z) = E_n\Psi_n(\mathbf{k}_{\|}, z) \quad (8)$$

where $V(z)$ represents the confining potential profile seen by the electron. In the direction parallel to the interface, k is a good quantum number, and the solution has a general form

$$\Psi^n_{electron} = \phi_n(z)u_o(r)e^{i\mathbf{k}_{\|}\cdot\rho} \quad (9)$$

where $\phi^n(z)$ is the electron envelope functions for the nth subband in the one dimensional problem, and $u_o(r)$ are the zone center Bloch functions. By substituting equation (9) into equation (8), we are left with a one dimensional Schrödinger equation for the envelope functions in which we use the prependicular electron effective mass. The eigen energies which result from the solution to this equation will be the minima of the subbands which are parabolic and characterized by the parallel effective mass. Note that the effective mass can change across interfaces from one material into another. This effect is easily included in the formalism if the Schrödinger equation is solved using finite difference techniques.

The hole states are much more complicated because of the four fold degeneracy at the zone center. The Kohn Luttinger hamiltonian can be used to describe the hole bands in a confining potential, except k_z must be treated as an operator ($k_z = -i\frac{\partial}{\partial z}$) so that the matrix elements listed in equation (5) becomes

$$\begin{aligned} H_{hh} &= -\frac{\hbar^2}{2m_o}\left[(k_x^2+k_y^2)(\gamma_1+\gamma_2) - (\gamma_1-2\gamma_2)\frac{\partial^2}{\partial^2 z}\right] \\ &\quad +V(z)+\frac{1}{2}\delta_{sh} \\ H_{lh} &= -\frac{\hbar^2}{2m_o}\left[(k_x^2+k_y^2)(\gamma_1-\gamma_2) - (\gamma_1+2\gamma_2)\frac{\partial^2}{\partial^2 z}\right] \\ &\quad +V(z)-\frac{1}{2}\delta_{sh} \\ c &= \frac{\sqrt{3}\hbar^2}{2m_o}\left[\gamma_2(k_x^2-k_y^2) - 2i\gamma_3 k_x k_y\right] \\ b &= \frac{\sqrt{3}\hbar^2}{m_o}(-k_y - ik_x)\gamma_3\frac{\partial}{\partial z} \end{aligned} \quad (10)$$

Here, δ_{sh} is the shear splitting discussed earlier. Analogously to the electron problem where the perpendicular effective mass was varied across interfaces to reflect different material characteristics, in the hole problem, the Kohn Luttinger parameters can also be so varied.

The general solution to this equation is slightly more complicated then for the electron case. In the electron case, the 'z' dependent part of the wavefunction, which we called the envelope function, and the in-plane radial portion of the wavefunction are strictly separable. Because of this, the envelope function varied with 'z', the real space dimension perpendicular to the interface, but not with $k_{\|}$. This allows us to easily calculate the charge distribution along the 'z' direction. For the hole case, the two variables in Schrödinger's equation are not strictly separable. Because of this, there may be some k-space dispersion of the envelope function. The general solution for the hole subbands can be written

$$\Psi^n_{hole} = \sum_\nu \phi^\nu_n(\mathbf{k}_{\|}, z)u^\nu_o(r)e^{i\mathbf{k}_{\|}\cdot\rho} \quad (11)$$

Here, $\phi^\nu_n(\mathbf{k}_{\|}, z)$ is the envelope function for the nth band which, as was just remarked, can be a function of **k** as well as z. ν is an index representing the different angular momentum states and, $u^\nu_o(r)$ are the zone center Bloch functions for the ν component of the wavefunction.

II.c The Charge Control Model

The potential profile, $V(z)$, in the above equations is obtained from the one dimensional Poisson equation,

$$\nabla^2 V(z) = -\frac{\rho(z)}{\epsilon(z)} \quad (12)$$

As indicated by equation (12), we can account for changes in material parameters by changing ϵ across interfaces. The charge density, $\rho(z)$, is the sum of the doping charge, the free charge, and the quantum confined charge. This can be written as

$$\rho(z) = N_d(z) - N_a(z) - n_{free}(z) + p_{free}(z) - \sum_i n_i\phi_i^*(z)\phi_i(z) \quad (13)$$

where N_a and N_d are the doping levels, n_{free} and p_{free} are the free carrier concentrations calculated by Fermi Dirac statistics, and the sum is over i two dimensionally confined subbands in which the occupation is n_i (or p_i for the hole case). In equation (13), we have written ϕ as a function of 'z' only. As discussed above, this is the readily available form of the solution for the electron case. For the hole case, however, to be strictly correct we would have to integrate over the band occupation in all of $\mathbf{k}_{\|}$ space to obtain the pure z dependence of the envelope function. In practice, this would take excessive computer time. To get around this problem, we introduce the approximation that after integrating out the **k** dependence of the envelope function, the result would be similar to the envelope function at **k**=0. That is,

$$|\phi_i(z, \mathbf{k}=0.)|^2 \approx \frac{\int_{-\infty}^{E_i} g_i(E)f(E)\,|\phi_i(z,E)|^2\,dE}{\int_{-\infty}^{E_i} g_i(E)f(E)dE} \quad (14)$$

where E_i is the maximum energy in the ith subband, $f(E)$ is the Fermi distribution function for holes, ϕ has been written in terms of energy rather then momentum (the relationship coming directly from the subband dispersions), and g_i is the subband density of states which is given by

$$g_i(E) = \frac{1}{4\pi^2}\frac{dA_i(E)}{dE} \quad (15)$$

where $A_i(E)$ is the area in k space contained by subband i at energy E.

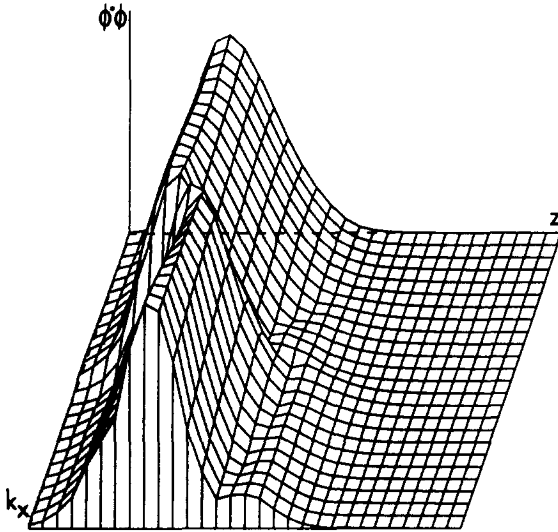

Figure 3: k-space dispersion of the squared magnitude of the envelope function. Note the small second hump towards the front of the figure indicating that the state has become mixed and now includes some of the first excited state.

The justification for using the approximation of equation (14) comes from the fact that the calculated dispersion of the envelope function does not vary strongly with **k** close to the zone center where most of the carriers will be. Figure 3 shows an example of a calculated dispersion of the envelope function. Depicted in figure 3 is the dispersion of the lowest $\Phi_{\frac{3}{2}\frac{-3}{2}}$ subband. The marked change in the dispersion comes at a point where the subband passes very close to the first excited $\Phi_{\frac{3}{2}\frac{3}{2}}$ subband. After this point, we can see that a small amount of the first excited state is mixed into the band as evidenced by the existence of a small second hump in the wave function. As can be seen, however, close to the zone center the envelope function does not change dramatically. Our calculations show that even though the envelope functions do change dramatically in some places, especially where two bands come close to each other in energy or cross each other, the total quantum confined charge distribution given by the sum in equation (13) is essentially unaltered by the approximation.

In order to determine the subband occupations, n_i or p_i, one has to determine the density of states in each subband, and integrate this multiplied by the Fermi distribution function. As with everything else, this is much easier to do in the electron case. In the electron case, the subbands are parabolic and can be characterized by a constant effective mass. Because of this, the density of states is a constant above the subband minimum energy, E_i. The integration of a constant multiplied by the Fermi distribution can be carrier out analytically giving the occupation in each electron subband to be

$$n_i = \frac{m_{\parallel}^*}{\pi\hbar^2} kTln\left[1 + exp\left(\frac{(E_i - E_F)}{kT}\right)\right] \qquad (16)$$

In the hole case, the subbands are very nonparabolic and, therefore, the density of states will not be a constant. Because of this, equation (15) must be used to numerically find the density of states in each band. This will then have to be numerically multiplied by the Fermi distribution function and intergated in order to determine the subband occupation. Due to this, the computer time involved in the solution of the p-type MODFET is quite significantly higher then the n-type MODFET.

One final aspect of the formalism merits discussion. This is the method which we use to account for free charge. Away from the quantum well where the carriers are not bound, the density of free electron or hole states takes on its normal form which is parabolic with energy. The density of occupied free carrier states, or the density of free carriers, can be calculated by evaluation of a half order Fermi integral. Inside of the quantum well the states below some confining energy will be two dimensional and will have the characteristics described above. However, even in the spatial location of the quantum well, there will be free carrier states with energies above the energy of the confining potential. We have accounted for these states be assuming that the parabola of free carrier states begins at the top of the confining potential instead of at the conduction band as is does in non-confined regions. Figure 4 conceptually shows this distribution of free and confined states at a position inside of the quantum well.

The outcome of the solution of the above equations is a full charge control model of the device, and properties of the two dimensional carrier gas in terms of masses, subband levels, subband occupations, etc. These results will be discussed in the following section.

III. RESULTS

In order to compare the two popular pseudomorphic materials systems in use today, we applied our model for a n-type MODFET to two similar structures one with a GaAs substrate, (the other with an InP substrate). The structure of the devices simulated was as follows : a thick buffer of $Al_{0.3}Ga_{0.7}As$ ($Al_{0.52}In_{0.48}As$), 400Å of GaAs ($In_{0.53}Ga_{0.47}As$), a 100Å thick layer of $In_xGa_{1-x}As$ ($In_{0.53+x}Ga_{0.47-x}As$) in which the excess In fraction, x was varied from 0 to 12 percent to simulate different

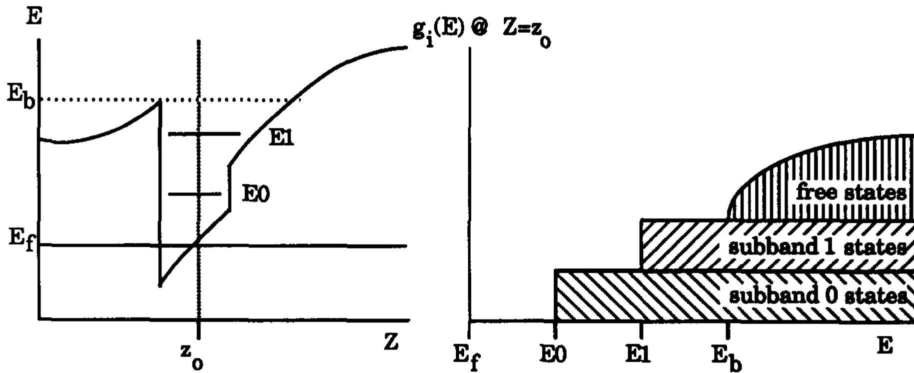

Figure 4: Conduction band profile and density of states at a point inside of the confining well. The free electron states do not appear until above the confining potential.

strains, a 100Å spacer of $Al_{0.3}Ga_{0.7}As$ ($Al_{0.52}In_{0.48}As$), a 200Å donor layer of $Al_{0.3}Ga_{0.7}As$ ($Al_{0.52}In_{0.48}As$) doped at $2 \cdot 10^{18}/cm^3$, a 100Å $Al_{0.3}Ga_{0.7}As$ ($Al_{0.52}In_{0.48}As$) cap layer, and then the gate. In both cases, the Schottky barrier height was taken to be 0.8 volts, and the band offsets were modeled at $\Delta E_c/\Delta E_v$ = 65:35. All of the n-type MODFET results presented here were done for 300°K.

Our model for the n-type MODFET yields the conduction band potential profile, the charge profile, for both free and two-dimensionally confined charge, and the subband energies. In figures 5 and 6 we show some of the results which our model predicts. First, we investigated the effects of adding indium to the channel on the sheet charge concentration. In figure 5, we show the two dimensional sheet charge density as a function of the excess indium concentration in the channel of the device for MODFETs made on GaAs and InP substrates. As can be seen, the increase in the sheet charge concentration is modest. These results are supported by the experimental work of Ng et al[10] who fabricated a series of devices on an InP substrate which are very similar to the structures which we modeled. The measured sheet charge densities in these devices showed little variation with strain, and varied about $1.33 \cdot 10^{12}/cm^2$, which is very close to the results of our model as shown in figure 5.

Another interesting parameter which the model can easily model is charge confinement. Two types of confinement, both of which are related, were studied, confinement in the lowest energy subbands, and spatial confinement within the strained channel region. Energy confinement is controlled in large part by the difference

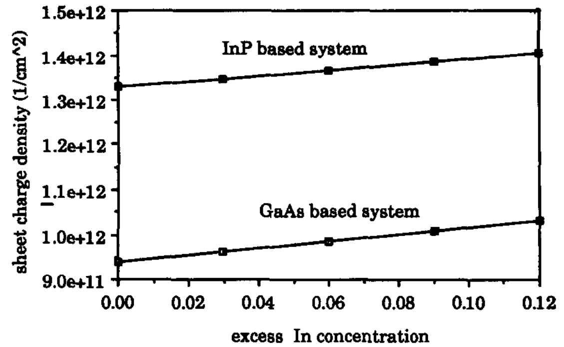

Figure 5: Increasing the Indium concentration in the channel increases the two dimensional sheet charge density.

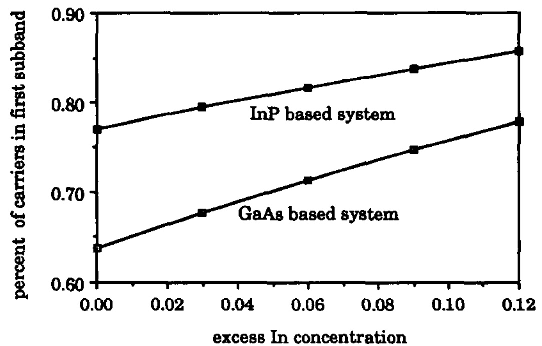

Figure 6: Increasing the strain in the channel creates a potential well into which the the ground state subband falls. This increases the confinement of the electrons in the ground state.

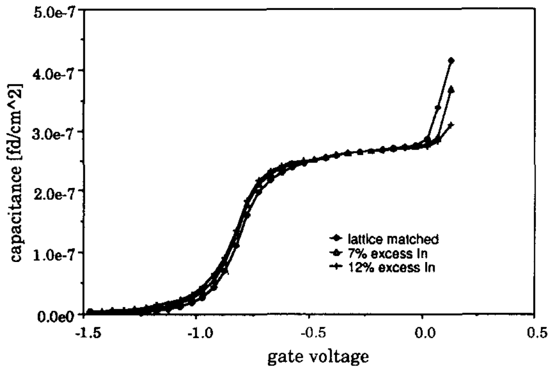

Figure 7: Capacitance voltage profile of lattice matched and strained MODFETs on an InP substrate. The addition of excess In in the channel has not had a large effect on the C-V curves.

in energy between the subbands. Both types of confinement can strongly effect carrier mobility. Mori and Ando[11], in a theoretical treatment of transport in superlattices, predicted that mobility will be several times less in even the first excited band then it is in the ground state. Spatial confinement can also have a negative effect on mobility because the carrier mass is generally much lower in the strained channel then it is in the barrier, or even in the substrate. Figure 6 shows the confinement of the electrons in the lowest energy subband. As can be seen, a substantial improvement in carrier confinement can be achieved with the addition of excess indium into the channel. A careful analysis of the model shows that the effect of the strain is to create a potential well in which only the first subband will reside. Thus, the difference in energy between the bottom of the first subband and the second subband is increased with added excess indium, and this creates better energy confinement. Spatial confinement is very much related to energy confinement as the higher energy subbands will be less spatially confined, however, the reduced carrier mass brought on by the higher mole fraction of indium will act to spread out each of the subbands spatially.

We also used our model to calculate the C-V characteristics of a pseudomorphic MODFET at different strains. Figure 7 shows the calculated capacitance-voltage profile for the InP based device with three different excess In concentrations. The effects of strain on the C-V profile, as can be seen, are small. Because of this, it may

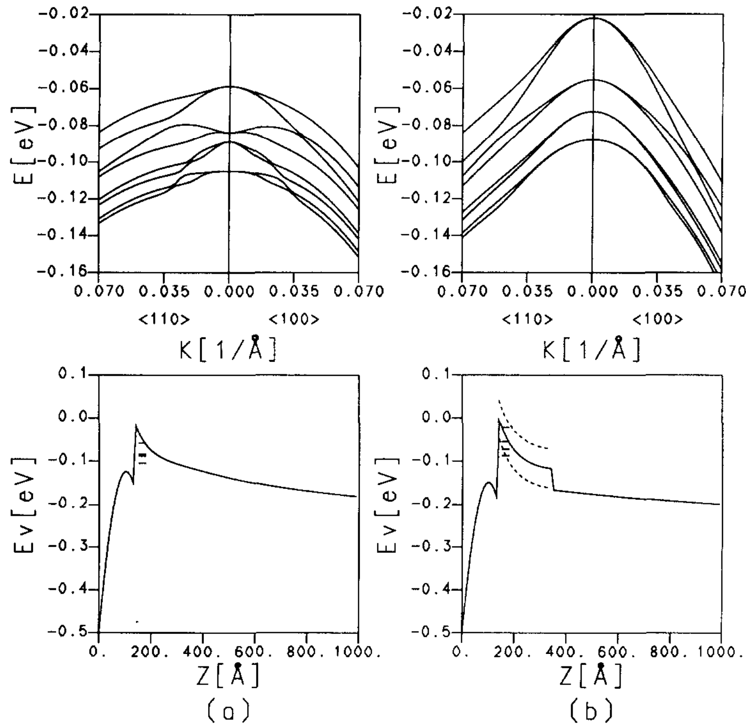

Figure 8: Hole subband dispersions and valence band profiles foe a) a lattice matched and b) a strained p-type MODFET. The dashed lines in the valence band of part b) indicate the effective valence band profile for the light and the heavy holes which have been split by strain.

Table 3: Results of the simulation of lattice matched and strained p-type MODFETs. Note the significant lowering of the overall effective mass and the improved confinement in the strained channel device.

Temp. (°K)	subband #	GaAs channel $n_s \cdot 10^{11}$	GaAs channel m^*_{dos}	GaAs channel E_n - E_F (meV)	GaAs channel state	$In_{0.20}Ga_{0.80}As$ channel $n_s \cdot 10^{11}$	$In_{0.20}Ga_{0.80}As$ channel m^*_{dos}	$In_{0.20}Ga_{0.80}As$ channel E_n - E_F (meV)	$In_{0.20}Ga_{0.80}As$ channel state
300	0	2.90	0.549	-58.7	HH0	3.83	0.199	-22.0	HH0
	1	2.18	0.411	-58.7	HH0	2.86	0.149	-22.0	HH0
	2	1.44	0.701	-83.9	LH0	1.61	0.268	-55.2	HH1
	3	1.20	0.585	-83.9	LH0	1.39	0.230	-55.2	HH1
	4	0.76	0.444	-88.7	HH1	0.74	0.234	-72.5	HH2
	5	0.68	0.395	-88.7	HH1	0.68	0.215	-72.5	HH2
	6	0.52	0.557	-105.	HH2	0.48	0.271	-87.7	HH3
	7	0.47	0.506	-105.	HH2	0.46	0.258	-87.7	HH3
	total	10.15	0.526			12.05	0.208		
77	0	4.44	0.536	-1.31	HH0	4.71	0.125	17.6	HH0
	1	2.16	0.261	-1.31	HH0	3.87	0.103	17.6	HH0
	2	0.94	1.015	-17.7	LH0	0.79	0.124	-3.49	HH1
	3	0.57	0.621	-17.7	LH0	0.75	0.118	-3.49	HH1
	4	0.28	0.388	-19.4	HH1	0.19	0.145	-15.3	HH2
	5	0.24	0.333	-19.4	HH1	0.18	0.141	-15.3	HH2
	6	0.17	0.567	-25.3	HH2	0.03	0.271	-31.9	HH3
	7	0.14	0.481	-25.3	HH2	0.03	0.251	-31.8	HH3
	total	8.97	0.514			10.58	0.118		

be difficult to use C-V profiling as a tool to characterize strain.

In the p-MODFET, the inclusion of excess indium into the channel can have very different effects then in the n-MODFET. In the n-MODFET, strain slightly altered the bandgap and the effective mass. The biggest effect of strain was to create a potential well in which the lowest subband rested, and this improved confinement. In the p-MODFET, strain splits the heavy and the light hole bands. This splitting can significantly affect the intersubband coupling, and this can have very large effects on the subband effective masses. For the p-type MODFET, successful evaluation of our model yields the conduction band potential profile, the charge profile, for both free and two-dimensionally confined charge, the subband energies, and the subband dispersion relationships, or the effective masses. Figure 8 shows the valence band profiles and the subband dispersions for a strained and a lattice matched p-type device on a GaAs substrate. The structure which we chose to model was similar to the structure grown earlier and reported by Lee et al[3]. Part a of figure 8 shows the valence band profile and the subband dispersions for the lattice matched system. Notice the flat dispersions of the subbands indicating heavy effective masses and the small separation in energy between the subbands indicating poor confinement which would further lower mobility. This points out the problems associated with attempting to produce lattice matched p-type MODFETs. Part b of figure 8 shows the same plots when the channel is composed of an alloy of 20% indium. Note that the strain has split the light and heavy hole bands and resulted in much lighter hole subbands, which can be seen by the substantially higher curvature. Also, the subbands have separated in energy, and this should improve carrier confinement and increase mobility even further. The dotted lines in the valence band profile in part b of figure 8 represent the splitting between the light and the heavy hole band in the bulk states. Thus, the upper dotted line is the effective valence band profile for the heavy hole, and the lower dotted line is the effective valence band profile for the light hole. A summary of the results of these simulations is shown in table 3. As can be seen from the table, the overall reduction in the density of states effective masses can be very significant. Our model predicts that the overall effective mass will be 2.5 times lighter in the pseudomorphic MODFET at room temperatures, and 4.3 times lighter at liquid nitrogen temperatures. The effect is especially pronounced at lower temperatures because the confinement in the uppermost hole subbands increases.

In the pseudomorphic p-type MODFET, the bands are very non-parabolic, and tend to be the lightest at the center of the Brillouin zone. Because of this, the

more holes which are put into the band, the heavier the overall (averaged) hole effective mass will be. This may have slight detrimental effects on the transconductance of the p-type MODFET, but the magnitude of such an effect is difficult to estimate without a model of hole transport.

IV. CONCLUSIONS

In this paper, we addressed the charge control issues in n- and p-type pseudomorphic MODFETs using a versatle numerical formalism. The formalism is capable of studying arbitrary shaped potential wells. For the p-type MODFET, the formalism includes the effects of HH-LH coupling. In the case of n-type MODFETs, we find that improvement in carrier mobility can be expected due to better charge confinement as the In content of the channel is increased. For the 100Å strained channel, the sheet charge increase was found to be modest, although the fraction of carriers in the ground state increases considerably. The improved confinement effects should result in better overall device performance.

The p-MODFET simulation show very remarkable effects, the most important of which being the dramatic decrease in the two dimensional hole gas effective mass as the strain in the channel is increased. This effect is due to the splitting if the light and the heavy hole bands. The effects are in good agreement with the qualitative improvements observed experimentally in strained p-MODFETs, and the general formalism is expected to be useful in understanding and designing strained p-MODFETs.

Acknowledgement - This work was supported by the National Science Foundation(the MRG program)and by the US Army Research Office(grant No.DAAL03-87-K-0007).One of us,M.J.,gratefully acknowledges the generous support of the Eastman Kodak Company.

REFERENCES

1. H. Morkoç, T. Henderson, W. Kopp, C. Peng, Electronics Letters, 22, p. 578, 1986.
2. E. Jones, I. Fritz, J. Schirber, M. Smith, T. Drummond, Proceedings of the International Symposium on GaAs and Related Compopunds, p. 227, 1986.
3. T. Drummond, T. Zipperian, I. Fritz, J. Schirber, T. Plut, Applied Physics Letters, 49(8), p. 461, 1986.
4. C. Lee, H. Wang, G. Sullivan, N. Sheng, D. Miller, IEEE Electron Device Letters, 8(3) p.85, 1987.
5. M. Jaffe, J. Singh, Solid State Communications, 62(6) p. 399, 1987.
6. W. Harrison, Electronic Structure and the Properties of Solids, W. H. Freeman, 1980.
7. D. Brido, C. Sham. Physical Review B, 31(2) p. 888, 1985.
8. P. Lawaetz, Physical Review B, 4(10), p. 3460, 1971.
9. C. Kuo, S. Vong, R. Cohen, G. Stringfellow, Journal of Applied Physics, 57(12) p. 5428, 1985.
10. G. Ng, D. Pavlidis, M. Quillec, Y. Chan, M. Jaffe, J. Singh, submitted to Electronics Letters.
11. S. Mori, T. Ando, Journal of the Physical Society of Japan, 48(3), p. 865, 1980.